Indian Journal of Chemistry
Vol. 57A, Aug-Sept 2018, pp. 1151-1155

# Role of polyvinyl pyrrolidone as a capping agent in the synthesis of magnetite ($Fe_3O_4$) nanoparticles

Sujata Kumari[a], Neha Yadav[a], Debasree Ghosh[a], Chandra Mohan Srivastava[a, *] & Sudip Majumder[a, b, *]

[a]Department of Chemistry, Amity School of Applied Science, Amity University Haryana

[b]Centre for Nanoscience and Technology, Amity University Gurgaon (Manesar) 122 413, Haryana, India

Email: smsmajumder@ggn.amity.edu (SN)/ cmsrivastava@ggn.amity.edu (CMS)

*Received 7 June 2018; revised and accepted 2 August 2018*

Uncapped magnetite ($Fe_3O_4$) and magnetite capped with polyvinyl pyrrolidone (PVP) ($Fe_3O_4$-PVP) have been synthesized by a rapid, cost effective aqueous precipitation method. The nanoparticles are characterized by powder X-ray diffraction, scanning electron microscopy, Fourier transform infrared spectroscopy and UV spectroscopy. The role of PVP as a capping agent in the synthesis of magnetite nanoparticles has been investigated. Thermal stability and surface charge of the nanoparticles have been characterized by thermogravimetric analysis, differential scanning calorimetry (DSC) and zeta potential measurements. Results suggest that PVP as a capping agent reduces the grain size, regularizes the shape, and increases the crystallinity of $Fe_3O_4$ nanoparticles. Thermal stability and surface charge of $Fe_3O_4$-PVP nanoparticles are also significantly higher as compared to the uncapped $Fe_3O_4$ nanoparticles. Magnetic characterization by vibrating sample magnetometry of both $Fe_3O_4$ and $Fe_3O_4$-PVP nanoparticles indicates the superparamagnetic behavior of the nanoparticles.

**Keywords:** Nanoparticles, Magnetite nanoparticles, Ferrites, Superparamagnetism, Co-precipitation, Iron oxide, Polyvinyl pyrrolidone

Among the ever increasing list of nanomaterials, transition metal oxide nanoparticles have drawn significant attention from researchers due to their wide range of applications such as anticancer agents, antimicrobial agents, optical materials, absorbents, electronic and electrical materials, heat transfer fluids, magnetic materials and so on[1-6]. Magnetite ($Fe_3O_4$) nanoparticles are common ferrites having an inverse cubic structure that imparts it with unique long term magnetic properties due to transfer of electron between $Fe^{2+}$ and $Fe^{3+}$ on tetrahedral and octahedral sites. Magnetite ($Fe_3O_4$) has evoked a surge in research for its many possible applications, primarily due to its magnetic properties[7-9]. These magnetite nanoparticles have applications in the field of medicine, electronics, food, fuel cells, solar cells, batteries, better air quality, chemical sensors and fabric. Magnetite nanoparticles are being used to clean up carbon tetrachloride and arsenic pollution from groundwater[10-16].

A wide variety of methods have been reported for synthesis of $Fe_3O_4$ nanoparticles, including co-precipitation[17], sol-gel method[18], flow injection[19], electrochemical[20], solvothermal[21], hydrothermal[22], microwave-assisted[23], thermal decomposition of iron(III) acetylacetonate in tri(ethylene glycol), etc [24].

Most of the impressive properties of these nanoparticles are related to their small size. Synthesis of magnetite nanoparticles in discrete and pure phase still remains a challenge, as these nanoparticles have a strong tendency to agglomerate. However, the most common method to overcome this problem is to use suitable capping agents during synthesis. Different types of capping agents have been successfully utilized for the synthesis of magnetic nanoparticles. The standard capping agents used for the synthesis of nanoparticles are citrate[25], tannic acid[26], polyvinyl pyrrolidone (PVP)[27], polyethylene glycol (PEG)[28], polysaccharides[29], etc. However, further investigations are required to understand the actual effect of capping agents on the size, structure and properties of magnetite ($Fe_3O_4$) nanoparticles.

$Fe_3O_4$ nanoparticles are very difficult to synthesize in pure state as they tend to oxidize to $Fe_2O_3$. To address this issue, in the present study, we report a rapid and effective capping method for the size-controlled synthesis of magnetite ($Fe_3O_4$) nanoparticles using PVP as capping agents. This method yields magnetite nanoparticles with uniform size distribution. We have analyzed the size, shape, crystallinity, thermal stability and surface charge of both the uncapped $Fe_3O_4$ and $Fe_3O_4$-PVP nanoparticles. Additionally, the spectral behavior and magnetic properties of $Fe_3O_4$ and $Fe_3O_4$-PVP nanoparticles have also been determined.

## Experimental

All the chemicals were purchased from Merck India.

$Fe_3O_4$ nanoparticles were synthesized by a co-precipitation method using a mixture of $Fe^{2+}$ and $Fe^{3+}$ salts as precursor as described by earlier

researchers[27]. Briefly, 50 mL of 2 M $FeCl_3.6H_2O$ and 50 mL of 1 M $FeSO_4.6H_2O$ were mixed together and heated in 500 mL round bottom flask under nitrogen atmosphere and vigorous mechanical stirring. Once the temperature of the solution reached 80 °C, liquor $NH_3$ was added dropwise to the solution at a rate of 0.2 mL/min until the pH of the solution became 10–11. With the addition of $NH_3$, the solution slowly turned black, suggesting the formation of black magnetite ($Fe_3O_4$). The heating at 80 °C was continued for 1 h. Then the solution was allowed to settle in the dark for 3 h. Finally, $Fe_3O_4$ nanoparticles were collected with an external magnet and washed repeatedly with deionized water and ethanol and dried in oven at 60 °C for 1 h.

To synthesize $Fe_3O_4$-PVP nanoparticles, 3 g of PVP was added to the initial mixture along with precursor iron salts. A similar procedure as above was adopted uptil the aging process at dark for 3 h. Then, 10 mL hydrazine solution was added to it with heating at 60 °C .The solution was filtered and the black residue was washed repeatedly with deionized water. Finally, the product was dried in muffle furnace at 60 °C for 6 h to get $Fe_3O_4$-PVP nanoparticles.

Characterization of the nanoparticles was done as described by Pandey *et al.*[1] XRD measurements were made using a X-ray diffractometer (Ultima III Rigaku, Japan) with a Cu target slit of 10 mm with Cu-Kα radiation of wavelength 1.54 Å. For the FTIR analysis, the nanoparticles' samples were dried and ground with KBr pellets and analyzed on a Nicolet IR 200 (Thermo Electron Corp, US). For SEM analysis, a droplet of the solution of the magnetic nanoparticles was transferred to a clean glass slide (1 cm × 1 cm) and micrographs were taken randomly at various locations with the help of SEM (Carl Zeiss, Germany) at an accelerating voltage of 15 kV after gold coating. Thermal gravimetric studies were carried out using a Pyris Diamond TG/DTA instrument (Perkin-Elmer, Singapore) operating under nitrogen atmosphere (150 mL/min). A Platinum crucible was used with alpha-alumina powder as reference. Zeta potential was measured using a Zetasizer instrument (Zetasizer Nano ZS, Malvern Instruments, UK). Magnetic characterization of the nanoparticles was done using a vibrating sample magnetometer (Lakeshore, VSM 7410)

## Results and discussion

The scanning electron micrographs of $Fe_3O_4$ nanoparticles are shown in Fig. 1. From Fig. 1, it is evident that the magnetite nanoparticles are small in size and distorted in shape. The size of the $Fe_3O_4$ nanoparticles as determined from SEM was found to be in the range of 50–120 nm (Fig. 1a) where the average diameter of the $Fe_3O_4$-PVP was found to be 60±10 nm (Fig. 1b). The rate of particle aggregation is a major factor that controls the morphology and structure (crystalline) of the nanoparticles. The size of the $Fe_3O_4$-PVP nanoparticles was smaller and they were more spherical and regular in shape due to the fact that PVP as capping agent provided controlled nucleation growth.

UV spectrum of $Fe_3O_4$ nanoparticles exhibited a general broad band in the region of 260–400 nm with a small peak at 284 nm followed by a faint shoulder at 364 nm (Supplementary data, Fig. S1). The UV spectrum of $Fe_3O_4$-PVP nanoparticles is almost identical to that of the uncapped sample. $Fe_3O_4$-PVP exhibits a broad band in the same range of 260–400 nm with the peak at 281 nm and the shoulder appearing at

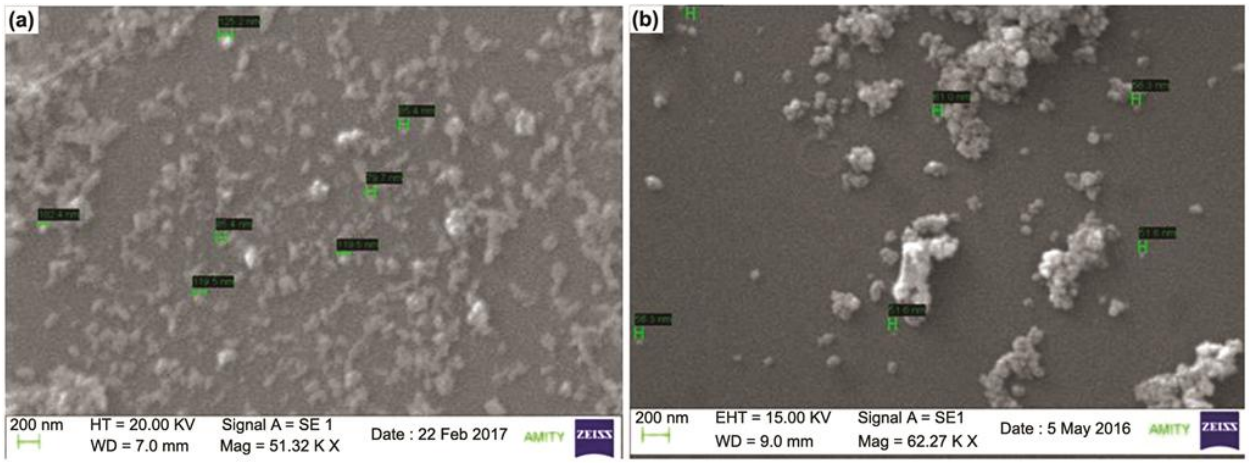


Fig. 1 — SEM micrographs of (a) $Fe_3O_4$, and, (b) $Fe_3O_4$-PVP nanoparticles.

the same position. This shows that PVP capping has a negligible effect on the UV spectrum of $Fe_3O_4$ nanoparticles, which has also been reported by other researchers[30].

X-ray diffractograms of $Fe_3O_4$ and $Fe_3O_4$-PVP are shown in Fig. 2. X-ray diffractogram of $Fe_3O_4$ nanoparticles shows a diffraction peak at $2\theta = 35.7°$, reflected from the (220) plane corresponding to the spinel phase of the $Fe_3O_4$ nanoparticles.

XRD peaks of $Fe_3O_4$-PVP at $2\theta = 32.22°$, 35.52°, 43.33°, 63.11° were found to concur with the values reported in literature[30-33] and match well with JCPDS card no. 19-0629. The average size of the magnetite nanoparticles was calculated from full width at half maxima of (220) diffraction reflection using Debye-Scherer equation. Average size of native $Fe_3O_4$ and $Fe_3O_4$-PVP were found to be 30 nm and 20 nm respectively. From the Fig. 2b, it is clear that the peaks became sharper, more distinct and prominent in magnetite $Fe_3O_4$-PVP as compared to the uncapped $Fe_3O_4$ nanoparticles. This also suggests the significant increase in crystallinity in $Fe_3O_4$-PVP, as compared to the uncapped ones which have a higher noise (and seemingly higher amorphous population content).

FTIR spectra of $Fe_3O_4$ and $Fe_3O_4$-PVP nanoparticles are depicted in Fig. 3. Both the spectra show a broad peak in the region of 3000–3300 $cm^{-1}$ due to O-H stretching of the adsorbed $H_2O$ molecules[30-33]. The peak at 1620 $cm^{-1}$ for both the uncapped and $Fe_3O_4$-PVP molecules represents the O-H bending. For the uncapped $Fe_3O_4$ and $Fe_3O_4$-PVP, a sharp doublet is observed in the region of 900–800 $cm^{-1}$. These doublets appear due to out-of-plane O-H vibration[24]. Uncapped $Fe_3O_4$ exhibits two other strong peaks at 630 $cm^{-1}$ and 430 $cm^{-1}$ respectively, corresponding to vibrations at tetrahedral and octahedral complexes. All these bands are due to different Fe-O lattice vibrations. The peak at 620 $cm^{-1}$ is due to Fe-O stretching vibration at the tetrahedral cluster, whereas the peak at 430 $cm^{-1}$ is due to vibration at the octahedral cluster. However, for $Fe_3O_4$-PVP nanoparticles the peaks are at 590 $cm^{-1}$ and 439 $cm^{-1}$ respectively, and represent the stretching vibration mode of Fe-O bond in $Fe_3O_4$-PVP at the

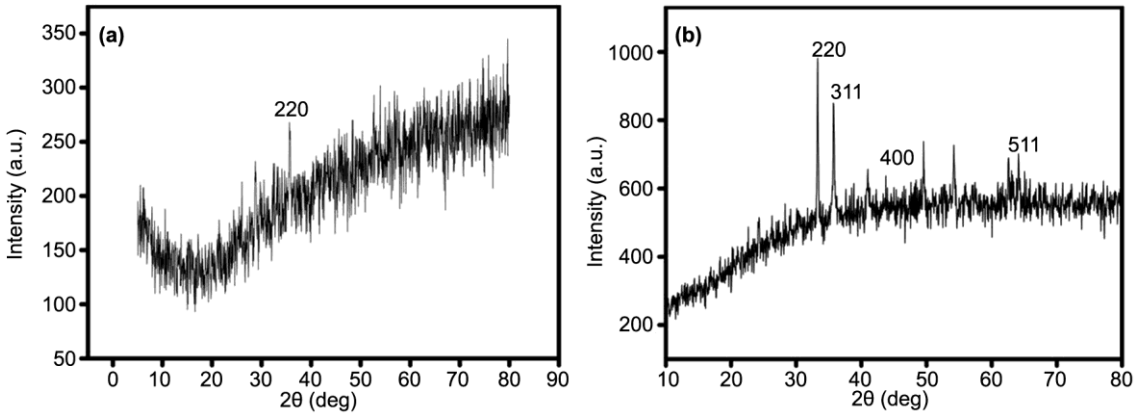


Fig. 2 — XRD pattern of (a) $Fe_3O_4$, and, (b) $Fe_3O_4$-PVP nanoparticles.

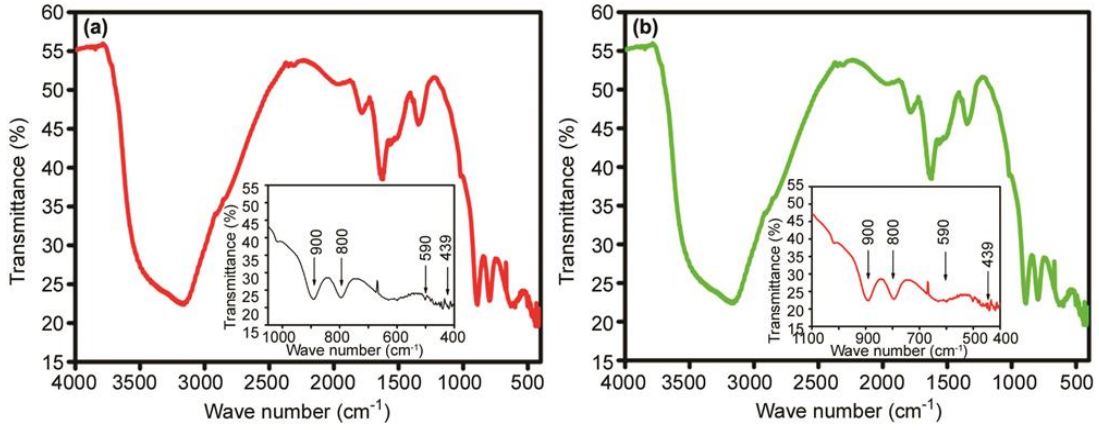


Fig. 3 — FTIR spectra of (a) $Fe_3O_4$, and, (b) $Fe_3O_4$-PVP nanoparticles. [Insets: Peaks in the range of 400–1100 $cm^{-1}$].

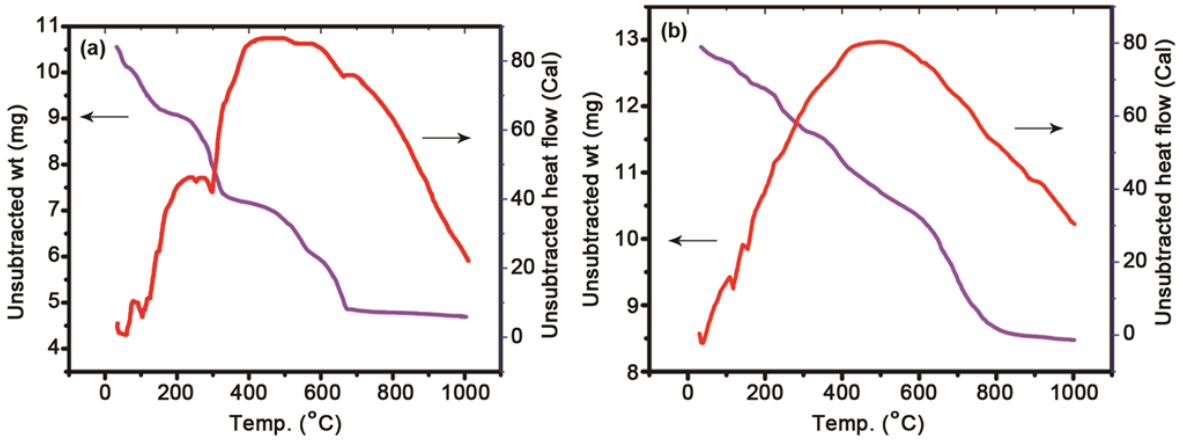


Fig 4 — TGA-DSC profile of (a) $Fe_3O_4$, and, (b) $Fe_3O_4$-PVP nanoparticles.

tetrahedral and octahedral sites. FTIR spectra suggest the formation of an inverse spinel magnetite structure. These observations are similar to those reported by other researchers[31-33]. Findings of XRD analysis are also reconfirmed by FTIR data.

Magnetic characterization of the nanoparticles was done by vibrating sample magnetometry (VSM) analysis. The plots of magnetization (*M*) versus applied field (*H*) of uncapped $Fe_3O_4$ nanoparticles and $Fe_3O_4$-PVP nanoparticles respectively are shown in Fig. S2 (Supplementary data).

The *M-H* plots of both the nanoparticles show when the coercivity absence of hysteresis was zero, indicating that these magnetic nanoparticles are superparamagnetic in nature[22-24]. On increasing the applied magnetic field from 0 G to 10000 G, the magnetization increased sharply and became nearly saturated at about 10000 G.

$Fe_3O_4$ nanoparticles and $Fe_3O_4$-PVP nanoparticles possess saturation magnetization (Ms) values of 0.26788 emu $g^{-1}$ and 0.26706 emu $g^{-1}$ respectively. The value of the saturation magnetization (Ms) for $Fe_3O_4$-PVP is slightly less than that of the uncapped $Fe_3O_4$ due to smaller particle size of $Fe_3O_4$-PVP. Retentivity (17.524) and coercivity (59.686) of $Fe_3O_4$-PVP nanoparticles are also significantly less than that of uncapped $Fe_3O_4$ (25.627 and 77.280 respectively).

TGA profiles suggest an initial 13% weight loss for uncapped $Fe_3O_4$ at ~150 °C, whereas for $Fe_3O_4$-PVP this weight loss is ~7%. This weight loss is due to the evaporation of adsorbed $H_2O$ and precipitant molecule in nanoparticles surface (Fig. 4).

TGA thermograms suggest that maximum weight loss for both the $Fe_3O_4$ and $Fe_3O_4$-PVP nanoparticles occurs at ~600 °C. However, the % weight loss is significantly lower for $Fe_3O_4$-PVP as compared to uncapped $Fe_3O_4$ (Supplementary data, Table S1). This indicates that PVP as a capping agent imparts significant thermal stability to $Fe_3O_4$ nanoparticles.

DSC curve for $Fe_3O_4$ shows an initial endothermic peak ~150 °C, suggesting the loss of adsorbed solvent and precipitant molecules followed by a large exothermic peak ~470 °C representing crystallization temperature of uncapped $Fe_3O_4$ (Fig. 4), for $Fe_3O_4$-PVP the initial exothermic peak is nearly absent suggesting less adsorption of undesired solvent molecules in the presence of capping agents (results also supported by TGA data). However, the exothermic peak for crystallization temperature for $Fe_3O_4$-PVP nanoparticles shifts to the slightly lower value of 460 °C (in accordance with XRD results, which also showed much higher level of crystallinity for $Fe_3O_4$-PVP as compared to uncapped $Fe_3O_4$.

Zeta potential was measured as an index of stability for the uncapped $Fe_3O_4$ and PVP capped $Fe_3O_4$ nanoparticles. The values recorded were +24.6 mV and +25.2 mV respectively. High positive value of Zeta potential shows the good colloidal stability of the synthesized nanoparticles. A slightly higher zeta potential of $Fe_3O_4$-PVP as compared to $Fe_3O_4$ suggests increase in stability of the nanoparticles with PVP capping. Additionally, the PDI values of uncapped $Fe_3O_4$ (Supplementary data, Fig. S3(a)) and capped $Fe_3O_4$-PVP (Fig. S3(b)) were found to be 0.351 and 0.490 respectively. The higher value of PDI for $Fe_3O_4$-PVP suggests a narrower size distribution for capped magnetite ($Fe_3O_4$) nanoparticles over the uncapped nanoparticles. This result is also in accordance with XRD and SEM data.

In summary, the effect of PVP as a capping agent on the size, shape, crystallinity, thermal stability, magnetic properties and surface charge of $Fe_3O_4$ nanoparticles is reported. Our findings suggest that use of PVP as a capping agent reduces the size of $Fe_3O_4$ nanoparticles and increases its crystallinity significantly. It is suggested that the presence of PVP controls the nucleation and growth of $Fe_3O_4$ nanoparticles. Thermal stability of $Fe_3O_4$-PVP is also significantly higher as compared to that of the uncapped $Fe_3O_4$. FTIR spectra suggest the formation of inverse spinel structure for both uncapped $Fe_3O_4$ and $Fe_3O_4$-PVP nanoparticles. VSM measurements reveal superparamagnetic behavior of these nanoparticles, with a slightly reduced magnetic parameter values. A higher value of zeta potential for $Fe_3O_4$-PVP nanoparticles, suggests the higher colloidal stability of $Fe_3O_4$-PVP as compared to uncapped $Fe_3O_4$. The study shows that the use of PVP as a capping agent yields smaller sized and regular shaped $Fe_3O_4$ nanoparticles with higher crystallinity, and better thermal and colloidal stability. Superparamagnetic nature of $Fe_3O_4$ nanoparticles was also observed for both uncapped $Fe_3O_4$ and $Fe_3O_4$-PVP nanoparticles.

## Supplementary data

Supplementary data associated with this article are available in the electronic form at http://www.niscair.res.in/jinfo/ijca/IJCA_57A(8-9)1151-1155_SupplData.pdf.

## Acknowledgement

SM acknowledges SAIF, IIT Madras, Chennai, India, for their help in VSM data collection.

## References

1 Pandey N, Dhiman S, Srivastava T & Majumder S, *Chem Biol Interact*, 254 (2016) 221.
2 Vinardell M P & Mitjans M, *Nanomaterials*, 5 (2015) 1004.
3 Shi J B, Lee C W, Guo J W, Cheng M J, Wu C, Chen C J, Chen Y C, Lin Y T & Chang C C, *Mater Lett*, 61 (2007) 5268.
4 Grover V A, Hu J, Engates K E & Shipley H J, *Environ Toxicol Chem*, 31 (2012) 86.
5 Mock J, Klingebiel B, Köhler F, Nuys M, Flohre J, Muthmann S, Kirchartz T & Carius R, *Phys Rev Mater*, 1 (2017) 065407.
6 Dhiman S, Yadav D, Varshney N, Joon P, Das S & Majumder S, *V$^{th}$ Int Symp on Fusion of Sci & Tech, ID: 2016-ISFT*, 372 (2016) 51989.
7 Li F, Vipulanandan C & Mohanty K, *Colloids Surf A*, 223 (2003) 103.
8 Lin C R, Chu Y M & Wang S, *Mater Lett*, 60 (2006) 447.
9 Compean J M E, Ruiz F, Martinez J R & Gómez A H, *Mater Lett*, 62 (2008) 4248.
10 Song E Q, Hu J, Wen C Y, Tian Z Q, Yu X, Zhang Z L, Shi Y B & Pang D W, *ACS Nano*, 5 (2011) 761.
11 Ito A, Shinkai M, Honda H & Kobayashi T, *J Biosci Bioeng*, 100 (2005) 1.
12 Banobre Lopez M, Teijeiro A & Rivas J, *Rep Pract Oncol Radiother*, 18 (2013) 397.
13 Wang K, Yi C, Liu C, Hu X, Chuang S & Gon X, *Sci Rep*, 5 (2015) 1.
14 Pourzare K, Mansourpana Y & Farhadi S, *BRJ*, 3 (2016) 496.
15 Keyhanian F Shariati S, Faraji M & Hesabi M, *Arab J Chem*, 9 (2016) 348.
16 Bisht G & Neupane S, *Nanotech Env Eng*, 3 (2016) 8.
17 Lien H L, Jhuo Y S & Chen L H, *Environ Eng Sci*, 24 (2007) 21.
18 Xu J, Yang H, Fu W, Du K, Sui Y, Chen J, Zeng Y, Li M & Zou G, *J Magn Mater*, 309 (2007) 307.
19 Alvarez S, Muhammed M & Zagorodni A, *Chem Eng Sci*, 61 (2006) 4625.
20 Cabrera L, Gutierrez S, Menendez N, Morales P & Herrasti P, *Electrochim Acta*, 53 (2008) 3436.
21 Liu M & Kim K, *Mater Lett*, 63 (2009) 428.
22 Zhang J, Chen Y, Wang N & Shi W, *J Cryst Growth*, 310 (2008) 5453.
23 Hong Y, Pan T & Li Z, *J Magn Magn Mater*, 303 (2006) 60.
24 Maity D, Kale N, Ghanekar K, Xue M & Jun D, *J Magn Magn Mater*, 321 (2009) 3093.
25 Naeimi H & Nazifi Z S, *J Nanopart Res*, 15 (2013) 2026.
26 Cahyana A H, Pratiwi D & Ardiansah B, *Int Conf on Recent Trends in Physics IOP Conf Series, Mat Sci Eng*, 188 (2017) 1.
27 Arora O, *World J Eng Res*, 2 (2017) 81.
28 Arsalani N, Fattahi H & Nazarpoor M, *Polym Lett*, 4 (2010) 329.
29 Tai M F, Chin LW, Sharifah B & Hamid A, *J Nanomater*, 2 (2016).
30 Nidhin M, Indumathy R, Sreeram K J & Nair B U, *Bull Mater Sci*, 31 (2008) 93.
31 Rahman O U, Mohapatra S C & Ahmad S, *Mater Chem Phys*, 132 (2012) 196.
32 Saranya T, Parasuraman K, Anbarasu M & Balamurugan K, *Nano Vis*, 5 (2015) 149.
33 Gómez M E, Lopez J A, González F, Bonilla F A, Latinoamericana G Z R & Metalurgiay D, *J Nanofluids*, 30 (2010) 60.
34 Silva M F, Luiz A S, Oliveira D, Ciciliati A M, Michele K L, Ivashita F F, Fernandes D M, Adelina A, Hechenleitner W, Edgardo A G & Pineda A G, *J Nanomater*, (2017) ID 7939727.

## Announcement

## International Conference on Mathematical Methods, Modeling and Simulation in Chemical Sciences (6–8 December 2018)

The International Conference on Mathematical Methods, Modeling and Simulation in Chemical Sciences shall be held during 6–8 December 2018 at the SSN College of Engineering Kalavakkam, Chennai 603110, India. The conference is jointly organized by the Departments of Mathematics & Chemical Engineering, SSN College of Engineering, Chennai, India, and the Society of Advancement for Chemical Sciences & Education IGCAR, Kalpakkam, India.

The conference aims to bring together experts, researchers and postgraduate students working in mathematical and computational modeling in chemical sciences, technology and engineering. The topics to be covered include:

Numerical Methods; Stochastic Modeling & Reliability; ●Graph Theory & its Applications; ●Neural Networks & Data Analytics; ●Fuzzy Theory & its Applications; ●Continuum Mechanics; ●Computational Fluid Dynamics; ●Materials, Conversion & Storage of Green Energy; ●Green & Sustainable Chemistry; ●Computational Techniques in Separation Processes; ●Isotope Separation Processes; ●Migration of Toxic Chemical in Air & Ground; ●Transport of Radionuclides in Air & Ground; ●Thermodynamic Models; ●Chemical Reactivity Assessment & Control; ●Computational & Theoretical Chemistry; ●Process Equipment Design; ●Process Modeling, Simulation & Optimization; ●BioResources – Recent Developments; ●Application of Catalysis in Chemical Sciences; ●Photochemistry & Solar Chemistry; ●Environmental Science & Sustainable Chemistry; ●Micro-, Nano- & Biotechnology; ●Remediation of Contaminated Soil & Water.

Further information may be obtained from the conference website: www.ssnicmmsc2018.com